Journal of Adhesion Science and Technology
Publication details, including instructions for authors and subscription information:
http://www.tandfonline.com/loi/tast20

Dynamic Contact Stiffness of Adhesive Hertzian Contact

Jiayong Tian [a]
[a] Institute of Crustal Dynamics, China Earthquake Administration, P.O. Box 2855, Beijing 100085, P.R. China;, Email: chenlitedtian@yahoo.com.cn
Published online: 02 Apr 2012.

To cite this article: Jiayong Tian (2011) Dynamic Contact Stiffness of Adhesive Hertzian Contact, Journal of Adhesion Science and Technology, 25:10, 1087-1094, DOI: 10.1163/016942410X535028

To link to this article: http://dx.doi.org/10.1163/016942410X535028

///VSP/// *Journal of Adhesion Science and Technology 25 (2011) 1087–1094*

Journal of ADHESION SCIENCE and TECHNOLOGY
brill.nl/jast

Dynamic Contact Stiffness of Adhesive Hertzian Contact

Jiayong Tian *

Institute of Crustal Dynamics, China Earthquake Administration, P.O. Box 2855, Beijing 100085, P.R. China

Received in final form 29 April 2009; revised 3 March 2010; accepted 3 March 2010

Abstract

Based on the JKR and DMT models, dynamic contact stiffness of a rigid sphere against an adhesive semi-infinite solid is investigated by the consideration of dynamic contact deformation at the contact interface. The assumption of sufficiently small oscillating force yields a dynamic contact-pressure distribution of constant contact size, and then dynamic contact stiffness. It is found that except for the contact radius, two adhesive models predict the same expression of quasi-static contact stiffness and dynamic adhesive contact stiffness factor (DACSF). The influence of the oscillating frequency and specimen elasticity on the DACSF is discussed.

Keywords

Dynamic contact stiffness, adhesive model, dry laser cleaning, ultrasonic-atomic-force microscopy

1. Introduction

With the increasing development of microelectromechanical systems (MEMS) and nanoelectromechanical systems (NEMS), dynamic adhesive contact plays an important role in the manufacturability, operating performance, and reliability of these systems [1]. The resonance-type microscopies, for example, ultrasonic-atomic-force microscopy (UAFM) [2] and resonance ultrasound microscopy (RUM) [3–5], have been developed to quantitatively evaluate the elastic modulus and surface energy of thin-film systems and small volumes of materials by the resonance-frequency shifts of an oscillator. An applied biasing force and an adhesive force make the oscillator contact the specimen surface through a tip, and an oscillating force excites the megahertz vibration of the oscillator, which is attributed to a problem of dynamic adhesive contact. Besides, during the fabrication of MEMS and NEMS devices, the micron and sub-micron contaminated particles are inevitably adhered to the substrate by Van der Waals forces, which has a fatal influence on

* Tel./Fax: +86-(0)10-62913587; e-mail: chenlitedtian@yahoo.com.cn

 DOI:10.1163/016942410X535028

the performance of these devices as they advance toward smaller dimensions. In order to control these contamination, dry laser cleaning (DLC) technology has been developed to remove particles from the substrate [6–9]. The particle absorbs the radiation from a laser pulse, heats up, and expands. This rapid expansion yields gigahertz oscillations of the spherical particle on the substrate surface. If the momentum of the particle is great enough, it can overcome the adhesive force and become detached from the substrate surface. This situation also belongs to the category of dynamic adhesive contact.

In the present UAFM and DLC technologies, dynamic adhesive contact was usually modeled by a spring support, whose stiffness is given by the static JKR adhesive model [10] (which is valid for compliant, elastic, large tip radius and high surface energy) or the static DMT adhesive model [11] (which is applicable for stiffer samples, small tip radius and low surface energy). For the static JKR contact stiffness, there exist two different expressions in the literature. The one [12–15] is predicted from load–displacement curves, which form is different from that of Hertzian contact in the absence of adhesion. The other follows the form of Hertzian contact stiffness in the absence of adhesion [16, 17]. Wahl *et al.* [12, 13] studied the contact stiffness of a micro-scale probe with model poly, PDMS, elastomers by a depth-sensing nano-indenter under oscillatory loading conditions. The frequency of oscillatory loading is between 2 and 200 Hz, which corresponds to the quasi-static condition in UAFM and DLC technologies. Their experiments have revealed the difference between the measured quasi-static JKR contact stiffness and the theoretical static JKR contact stiffness predicted from load–displacement curves, where the measured quasi-static contact stiffness follows the form of Hertzian contact stiffness in the absence of adhesion. The measured quasi-static JKR contact stiffness approaches the punch contact stiffness of fixed contact size with the increase of the oscillating frequency. They attributed this discrepancy to the effect of viscoelasticity of the specimen on an oscillating crack tip in a JKR contact. However, their viscoelasticity model is only suitable for the quasi-static adhesive contact in UAFM and DLC technologies.

This paper has a two-fold purpose: firstly, to clarify the definition of the static and quasi-static JKR contact stiffnesses from the contact pressure distribution; and secondly, to investigate the dynamic contact stiffness of adhesive Hertzian contact, considering the dynamic contact deformation at the contact interface [18, 19], based on the JKR and DMT adhesive models.

2. Dynamic Adhesive Contact

In order to simplify the following analysis, we consider dynamic adhesive contact vibration between a rigid sphere of radius R against an elastic semi-infinite solid of Young's modulus E and Poisson ratio ν, which is shown in Fig. 1. A dynamic force $F + \delta F e^{i\omega t}$ excites the oscillation of the sphere, where the harmonic force δF is much smaller than the biasing force F or the adhesive force.

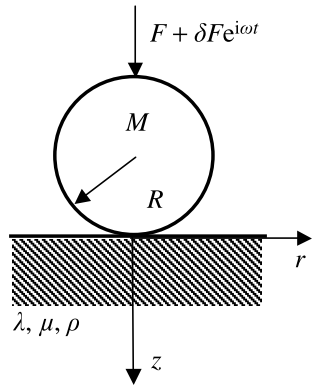

Figure 1. The forced vibration of a rigid sphere against an adhesive semi-infinite solid.

Firstly, the static adhesive contact is considered. The static JKR adhesive model gives the elastic contact pressure distribution ($p_{0(\mathrm{JKR})}(r)$), contact radius ($a_{(\mathrm{JKR})}$), and indentation ($w_{(\mathrm{JKR})}$) related to the work of adhesion $\Delta\gamma$, respectively, as [20]:

$$p_{0(\mathrm{JKR})}(r) = \frac{2a_{(\mathrm{JKR})}E^*}{\pi R}\sqrt{1 - r^2/a_{(\mathrm{JKR})}^2} - \sqrt{\frac{2\Delta\gamma E^*}{\pi a_{(\mathrm{JKR})}}}\frac{1}{\sqrt{1 - r^2/a_{(\mathrm{JKR})}^2}}, \quad (1)$$

$$a_{(\mathrm{JKR})} = \left(\frac{3R}{4E^*}\left(\sqrt{F + 3\pi\Delta\gamma R/2} + \sqrt{3\pi\Delta\gamma R/2}\right)^2\right)^{1/3}, \quad (2)$$

$$w_{(\mathrm{JKR})} = a_{(\mathrm{JKR})}^2/R - \sqrt{2\pi\Delta\gamma a_{(\mathrm{JKR})}/E^*}, \quad (3)$$

where $E^* = E/(1 - \nu^2)$. The static contact-pressure distribution in equation (1) includes the Hertzian-contact profile and the rigid-punch-contact profile induced by the surface energy. The static JKR contact stiffness can be expressed as:

$$K_{\mathrm{s(JKR)}} = \frac{\mathrm{d}F}{\mathrm{d}a}\frac{\mathrm{d}a}{\mathrm{d}w}. \quad (4)$$

Here the surface-energy-related contact radius should be involved in the differential of the contact force and the indentation in equation (4) results in two different form of static JKR stiffness [12–17]. If involved [12–15], the relationship for Hertzian contact without adhesion will not hold for the static JKR stiffness. Wahl's experiment [12] shows that when the rate of oscillating loading increases from 0 to 160 Hz, the contact stiffness will transform from the static contact stiffness to punch stiffness of fixed contact size, which means that static and quasi-static JKR contact stiffnesses are different. Therefore, we clarify the definition of the static and quasi-static JKR stiffness. For the static JKR contact stiffness, the contact radius in the surface-energy-related items of surface-energy-induced pressure distribution will be involved in the differential of the contact force and the indentation in equation (4). For the quasi-static JKR contact stiffness, the contact radius in the

surface-energy-related items should be the constant for the calculation of the contact stiffness in quasi-static loading conditions, which gives the quasi-static JKR contact stiffness $K_{\mathrm{qs(JKR)}}$ as:

$$K_{\mathrm{qs(JKR)}} = \frac{\mathrm{d}F}{\mathrm{d}w} = 2E^* a_{\mathrm{(JKR)}}. \tag{5}$$

The quasi-static JKR contact stiffness has the same form as Hertzian contact in the absence of adhesion.

The DMT adhesive model assumes that the adhesion forces do not change the Hertzian-contact-pressure profile, which gives the elastic contact pressure distribution ($p_{0\mathrm{(DMT)}}(r)$), contact radius ($a_{\mathrm{(DMT)}}$), and indentation ($w_{\mathrm{(DMT)}}$), respectively, as [11]:

$$p_{0\mathrm{(DMT)}}(r) = \frac{2a_{\mathrm{(DMT)}}E^*}{\pi R}\sqrt{1 - r^2/a^2_{\mathrm{(DMT)}}}, \tag{6}$$

$$a_{\mathrm{(DMT)}} = \left(\frac{3R}{4E^*}(F + 2\pi\Delta\gamma R)\right)^{1/3}, \tag{7}$$

$$w_{\mathrm{(DMT)}} = a^2_{\mathrm{(DMT)}}/R. \tag{8}$$

Therefore, the quasi-static DMT contact stiffness $K_{\mathrm{qs(DMT)}}$ also follows the Hertzian-contact expression, which is denoted as:

$$K_{\mathrm{qs(DMT)}} = 2E^* a_{\mathrm{(DMT)}}. \tag{9}$$

Secondly, we consider the case for the dynamic force $F + \delta F \mathrm{e}^{\mathrm{i}\omega t}$. Introducing the perturbation terms $\delta a \mathrm{e}^{\mathrm{i}\omega t}$ of contact radius a and neglecting higher-order terms, the dynamic contact pressure distribution for the JKR and DMT adhesive models can be expressed as the superposition of the corresponding quasi-static contact pressure distribution $p_0(r)$ and the same oscillating contact pressure distribution $\delta p(r)\mathrm{e}^{\mathrm{i}\omega t}$:

$$\delta p(r) = \frac{2E^*\delta a}{\pi R\sqrt{1 - r^2/a^2}}, \tag{10}$$

where contact radius a is $a_{\mathrm{(JKR)}}$ for JKR adhesive model and $a_{\mathrm{(DMT)}}$ for DMT adhesive model. In the deduction of dynamic contact pressure distribution for JKR adhesive model, the contact radius in the surface-energy-related items is also considered constant. The oscillating elastic contact force $\delta P \mathrm{e}^{\mathrm{i}\omega t}$ can be expressed as [19]

$$\delta P = \frac{4\pi a^2 E^* \delta a}{R}. \tag{11}$$

Thirdly, we consider the harmonic normal displacement $u_z(r, 0)$ at the contact interface of the semi-infinite solid of damping ratio ζ induced by the oscillating contact pressure distribution $\delta p(r)$, which can be expressed as [19, 21]:

$$u_z(r, 0) = \frac{4a\delta a N(r/a)}{R(1 - \nu)}, \tag{12}$$

where

$$N(\tilde{r}) = \int_0^\infty -\frac{\eta_2^2}{(1+2\mathrm{i}\zeta)^2}\sqrt{\eta^2 - \frac{1-2\nu}{2(1-\nu)}\frac{\eta_2^2}{(1+2i\zeta)^2}}\sin(\eta)J_0(\eta\tilde{r}) \Bigg/ \left(\left(2\eta^2 - \frac{\eta_2^2}{(1+2\mathrm{i}\zeta)^2}\right)^2 - 4\eta^2\sqrt{\eta^2 - \frac{1-2\nu}{2(1-\nu)}\frac{\eta_2^2}{(1+2\mathrm{i}\zeta)^2}}\sqrt{\eta^2 - \frac{\eta_2^2}{(1+2\mathrm{i}\zeta)^2}}\right)\mathrm{d}\eta,$$

and $\eta_2 = \frac{\omega}{\sqrt{\mu/\rho}}a$ is the normalized shear-wave number of the solid. If the contact radius is fixed, the η_2 will increase with the increase of the oscillating frequency.

Following the Hertzian contact theory, dynamic contact-displacement condition is provided, where the harmonic normal displacement $u_z(r,0)$ at contact interface is uniform and equals the harmonic indentation δw of the sphere:

$$u_z(r,0) = \delta w. \tag{13}$$

The oscillating-contact-pressure distribution can promise the uniform normal displacement at the contact interface for the static contact ($\omega = 0$). However, for the dynamic contact ($\omega > 0$), the harmonic normal displacement is impossible to keep uniform at the contact interface. So, following the procedure of Bycroft [22], an approximated oscillating-contact-displacement condition is given as:

$$\int_0^a \frac{u_z(r,0)r}{a\sqrt{a^2-r^2}}\,\mathrm{d}r = \delta w. \tag{14}$$

Here the weighted average displacement at the contact interface with respect to the oscillating contact pressure distribution equals the oscillating indentation. Thus, dynamic contact stiffness is defined as the ratio of the oscillating contact force to the oscillating indention:

$$K_\mathrm{d} = \frac{\delta P}{\delta w} = \frac{\pi E^*(1-\nu)a}{\int_0^1 (N(r)r/\sqrt{1-r^2})\,\mathrm{d}r}, \tag{15}$$

where contact radius a is $a_{(\mathrm{JKR})}$ for JKR adhesive model and $a_{(\mathrm{DMT})}$ for DMT adhesive model. In order to consider the characteristic of dynamic adhesive contact, dynamic adhesive-contact-stiffness factor (DACSF) κ_f related to the quasi-static adhesive-contact stiffness is introduced to be:

$$\kappa_\mathrm{f} = \frac{K_\mathrm{d}}{K_\mathrm{qs}} = \frac{\pi(1-\nu)}{2\int_0^1 (N(r)r/\sqrt{1-r^2})\,\mathrm{d}r}. \tag{16}$$

Here, dynamic JKR and DMT adhesive models follow the same expression for DACSF. Equation (16) indicates that DACSF is a complex number, whose real and imaginary parts represent the stiffness and energy dissipation of the vibration system, respectively.

3. Results and Discussions

It is observed from equation (16) that DASCF is only determined by the normalized shear-wave number η_2, Poisson's ratio ν, and damping ratio ζ of the solid. DASCF has the limit of $\kappa_f = 1 + 2i\zeta$ as $\eta_2 \to 0$, which corresponds to the quasi-static solution if $\zeta = 0$. In the experiment of Wahl *et al.* [12], the frequency of the oscillator is smaller than 200 Hz, and the contact radius is smaller than 20 μm, which means that η_2 is smaller than 3×10^{-6}. Therefore, it is reasonable that we attribute the model of Wahl *et al.* [12] to quasi-static model.

Figure 2 shows the influence of Poisson's ratio ν and the normalized wave number η_2 on DACSF. The real and imaginary parts of DASCF are shown in Fig. 2(a) and 2(b), respectively. The contact stiffness hardens with the increase of η_2 until it reaches the maximum at $\eta_2 \approx 0.589$. The maximum of the contact stiffness decreases as Poisson's ratio ν increases, which can be approximated as $1.1 - 0.0459\nu$. In UAFM and DLC technologies, typical operational frequencies are in the range of a few MHz to a few hundred MHz, and the contact radius ranges from about a few hundred nanometers to a few micrometers. The shear-wave velocity of most specimen is from 50 m/s to 3000 m/s, so the η_2 is smaller than 0.5. This means that in UAFM and DLC technologies, dynamic adhesive contact stiffness must be considered to investigate the contact vibration response in place of the quasi-static adhesive contact stiffness.

After the maximum, the contact stiffness will soften with the increase of η_2. At $\eta_2 = 2$, the contact stiffness is only one tenth of the quasi-static value. The energy dissipation increases with the increase of η_2 and decreases as Poisson's ratio ν increases.

4. Conclusions

In summary, the contact stiffness of dynamic adhesive Hertzian contact based on JKR and DMT adhesive model is presented from the consideration of dynamic contact deformation at contact interface. According to the surface-energy-related contact pressure distribution, the quasi-static contact stiffness for JKR adhesive model has been clarified to follow the form of Hertzian contact stiffness in the absence of adhesion. The dynamic contact stiffness for JKR and DMT adhesive models can be expressed as the product of the corresponding quasi-static contact stiffness and the same dynamic-contact-stiffness factor, which is influenced by the operational frequency of the oscillator and the Poisson ratio of the specimen. The dynamic-contact-stiffness factor will be more than unity in the operational frequency range of UAFM and DLC technologies. Therefore, the consideration of dynamic adhesive contact stiffness will benefit UAFM and DLC technologies.

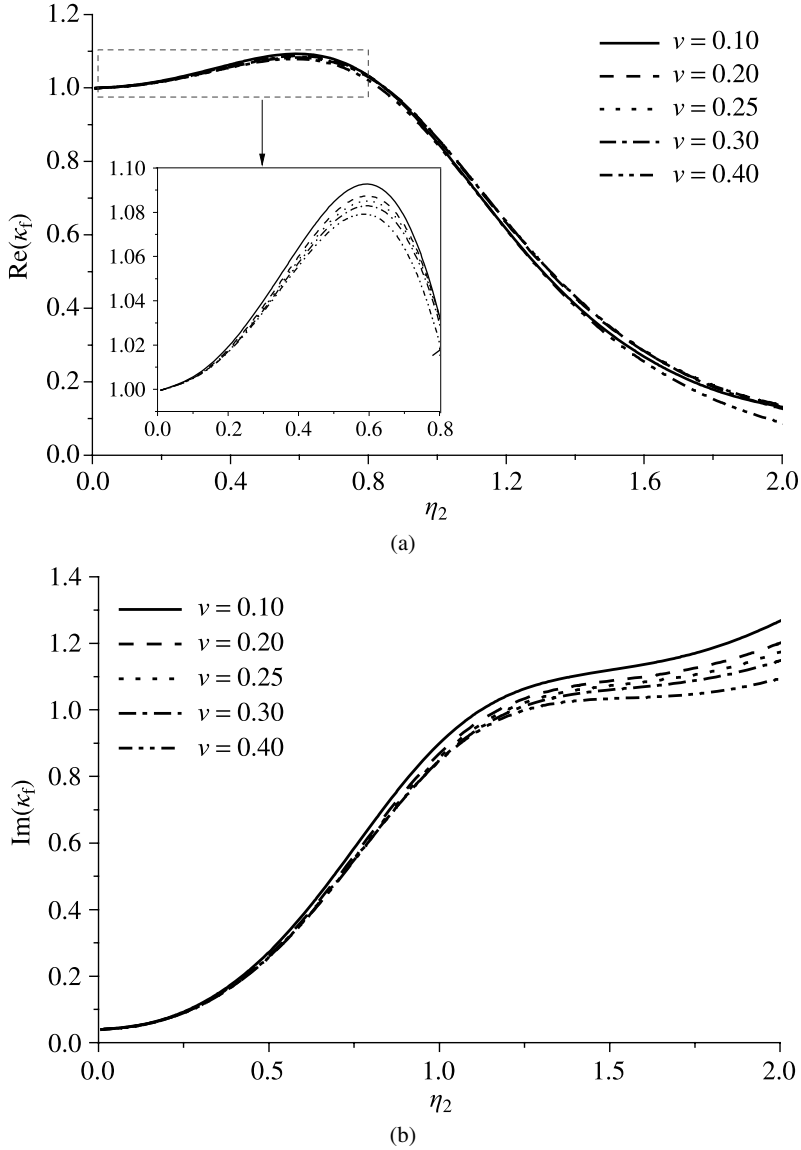

Figure 2. The influence of Poisson's ratio ν and normalized wave number η_2 on dynamic adhesive contact stiffness factor. (a) Real part. (b) Imaginary part.

Acknowledgements

A part of this study was supported by the National Natural Science Foundation of China (Nos. 10602053 and 50808170), research grants from Institute of Crustal Dynamics (No. ZDJ2007-2) and for oversea-returned scholar, Personnel Ministry of China.

References

1. C. D. Yeo, S. C. Lee and A. A. Polycarpou, *Review of Scientific Instruments* **79**, 015111–015111-8 (2008).
2. U. Rabe, J. Turner and W. Arnold, *Applied Physics A* **66**, S277–S282 (1998).
3. H. Ogi, J. Tian, T. Tada and M. Hirao, *Applied Physics Letters* **83**, 464–466 (2003).
4. J. Tian, H. Ogi, T. Tada and M. Hirao, *Journal of the Acoustical Society of America* **115**, 630–636 (2004).
5. J. Tian, H. Ogi, T. Tada and M. Hirao, *IEEE Transactions on Ultrasonics Ferroelectrics and Frequency Control* **55**, 499–502 (2008).
6. M. Mosbacher, H. J. Munzer, J. Zimmermann, J. Solis, J. Boneberg and P. Leiderer, *Applied Physics A: Materials Science and Processing* **72**, 41–44 (2001).
7. Y. W. Zheng, B. S. Luk'yanchuk, Y. F. Lu, W. D. Song and Z. H. Mai, *Journal of Applied Physics* **90**, 2135–2142 (2001).
8. S. Pleasants and D. M. Kane, *Journal of Applied Physics* **93**, 8862–8866 (2003).
9. B. S. Luk'Yanchuk, N. Arnold, S. M. Huang, Z. B. Wang and M. H. Hong, *Applied Physics A: Materials Science and Processing* **77**, 209–215 (2003).
10. K. L. Johnson, K. Kendall and A. D. Roberts, *Philosophical Transactions of the Royal Society of London* **A324**, 301–313 (1971).
11. B. V. Derjaguin, V. M. Muller and Y. P. Toporov, *Journal of Colloid and Interface Science* **53**, 314–326 (1975).
12. K. J. Wahl, S. A. S. Asif, J. A. Greenwood and K. L. Johnson, *Journal of Colloid and Interface Science* **296**, 178–188 (2006).
13. D. M. Ebenstein and K. J. Wahl, *Journal of Colloid and Interface Science* **298**, 652–662 (2006).
14. J. A. Greenwood and K. L. Johnson, *Journal of Colloid and Interface Science* **296**, 284–291 (2006).
15. O. Pietrement and M. Troyon, *Journal of Colloid and Interface Science* **226**, 166–171 (2000).
16. Y. P. Zhao, L. S. Wang and T. X. Yu, *Journal of Adhesion Science and Technology* **17**, 519–546 (2003).
17. X. Shi and Y. P. Zhao, *Journal of Adhesion Science and Technology* **18**, 55–68 (2004).
18. J. Tian, H. Ogi and M. Hirao, *Journal of Applied Physics* **95**, 8366–8375 (2004).
19. J. Y. Tian, H. Ogi and M. Hirao, *IEEE Transactions on Ultrasonics Ferroelectrics and Frequency Control* **51**, 1557–1563 (2004).
20. K. L. Johnson, *Proceedings of the Royal Society A: Mathematical, Physical and Engineering Sciences* **453**, 163–179 (1997).
21. C. J. Cornejo Córdova, *Ph.D. Thesis*, Technische Universiteit Delft (2002).
22. G. N. Bycrot, *Philosophical Transactions of the Royal Society of London* **A248**, 327–368 (1956).